Ab initio study of magnetic effects on diffusion in α-Fe

2004 J. Phys.: Condens. Matter 16 7033

(http://iopscience.iop.org/0953-8984/16/39/036)

INSTITUTE OF PHYSICS PUBLISHING JOURNAL OF PHYSICS: CONDENSED MATTER

J. Phys.: Condens. Matter **16** (2004) 7033–7043 PII: S0953-8984(04)78203-X

Ab initio study of magnetic effects on diffusion in α-Fe

Rodolfo Ariel Pérez[1,3] **and Mariana Weissmann**[2,3]

[1] Departamento de Materiales, Comisión Nacional de Energía Atómica, Avenida del Libertador 8250, 1429 Buenos Aires, Argentina
[2] Departamento de Física, Comisión Nacional de Energía Atómica, Avenida del Libertador 8250, 1429 Buenos Aires, Argentina

Received 22 March 2004, in final form 16 July 2004
Published 17 September 2004
Online at stacks.iop.org/JPhysCM/16/7033
doi:10.1088/0953-8984/16/39/036

Abstract

A deviation from the Arrhenius law in α-Fe self-diffusion and also in the diffusion of substitutional impurities is found experimentally. Below the Curie temperature the diffusion coefficients have lower values than those extrapolated from the paramagnetic region and the Arrhenius plot shows an upward curvature.

In this work we attempt to understand this behaviour from first-principles calculations. Formation and migration energies for self-diffusion and also for the diffusion of some substitutional impurities are calculated. Spin-polarized and non-spin-polarized calculations are assumed to approximately represent ferromagnetic and paramagnetic α-Fe respectively.

The calculations were performed using the WIEN97 code, with a supercell of 36 atoms which allows us to include both vacancies and impurities and therefore to study the migration along the $\langle 111 \rangle$ direction. The increment in the diffusion barrier due to the total magnetic alignment at 0 K, with respect to the paramagnetic case, is almost constant for non-magnetic impurities, as it is in the experiments, whereas for magnetic impurities it depends on the diffusing atom.

1. Introduction

The effect of magnetism on self-diffusion and vacancy mediated impurity diffusion in iron is an interesting field of research for both academic reasons and for its applications [1]. We shall be concerned in this paper with differences between magnetic and non-magnetic impurities. Some non-magnetic impurities such as Sn and Sb have been studied in our laboratory and results for magnetic impurities such as Co and Cr have been taken from the literature. All these elements are known to be substitutional diffusers.

[3] Member of the Carrera del Investigador Científico del CONICET.

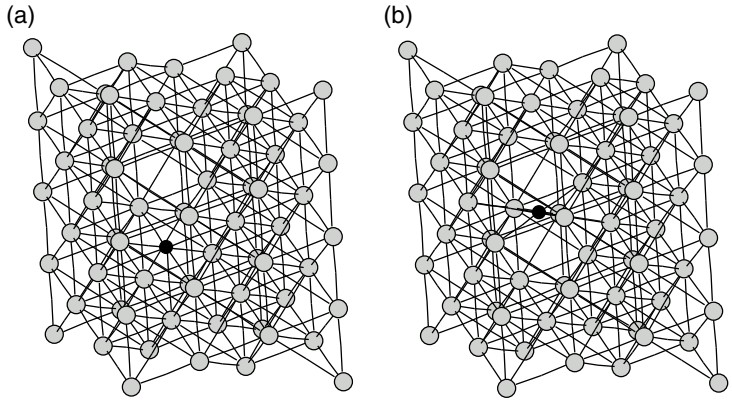

Figure 1. The supercell used in the calculations, showing the number of Fe atoms that separate the impurities when periodicity is imposed: (a) a substitutional impurity next to a vacancy; (b) an impurity at a saddle point.

The experimental results show in all cases a break in the Arrhenius plot at the Curie temperature and a soft upward curvature at lower temperatures. This curvature originates from an increment of the activation energy in the ferromagnetic state, which depends on temperature as the square of the spontaneous magnetization. We have observed that this increment is almost constant for the non-magnetic impurities and has different values for each magnetic impurity. The main point of this work is to find out whether this behaviour is also obtained when calculating migration and formation energies theoretically by *ab initio* methods. In the literature a simple Ising-type model is used to fit the experimental results [2], and we will also attempt to obtain the fitting parameters from these calculations.

The energy differences to be calculated are very small, but they can be obtained using *ab initio* methods, within the milliRydberg limit. Previous calculations [3, 4] were performed using other techniques, that allow larger unit cells and also a relaxation of the structure. It is interesting to compare those results with a more precise *ab initio* calculation, for an unrelaxed structure but with a reasonably large unit cell. For this purpose we evaluate the formation and migration energies of the vacancies close to substitutional impurities, using a periodic three-dimensional system consisting of repeated supercells with 36 atoms, that is, a 3% concentration of impurities and vacancies. A larger size of the unit cell in the $\langle 111 \rangle$ direction was chosen to obtain a rather dilute alloy (see figure 1), which makes the calculated results close to the experimental situation. Increasing the unit cell in the perpendicular direction would increase the number of atoms in the cell beyond our computational possibilities.

We have performed *ab initio* calculations for the magnetic (spin-polarized) and paramagnetic (non-spin-polarized) configurations, making the somewhat bold assumption that their diffusion properties may be comparable to those below and above the Curie temperature respectively.

2. Method of calculation

The electronic structure and total energies were obtained using the WIEN97 code [5] which is an implementation of the linearized augmented plane wave (FP-LAPW) method based on density functional theory. The local spin density approximation (LSDA) for exchange and correlation, as improved by Perdew *et al* [6] for the GGA case, was used because it gives

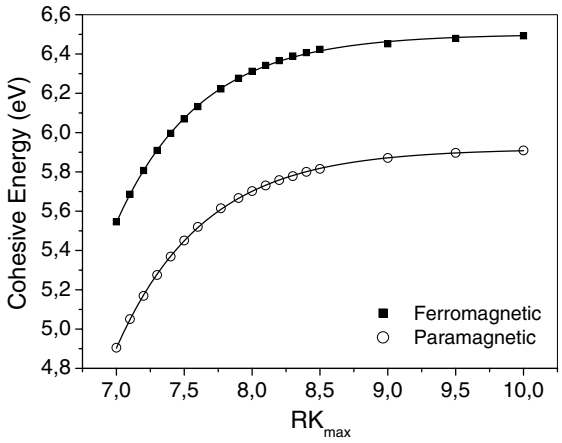

Figure 2. Calculated cohesive energy versus RK_{max} for pure bcc Fe.

the best results for the lattice parameter and cohesive energy of bcc Fe. Scalar-relativistic effects were included in the calculation; the **k**-point sampling of the Brillouin zone (BZ) was at 150 points. The atomic sphere (muffin-tin) radii were taken as 2 au for 3d metals and 2.2 au for 4d metals. The lattice parameter for bulk pure bcc iron was obtained by energy minimization and this value (5.42 au) was used in the rest of the calculations.

A well known problem in this type of calculation is the number of plane waves required for convergence, which determines the size of the matrices to be diagonalized. The adimensional parameter RK_{max}, which controls the size of the plane wave basis sets in the WIEN97 code, is defined as the product of the plane wave cut-off and the smallest atomic sphere radii ('muffin-tin' radii). The total cell energy changes when RK_{max} increases, until it reaches a converged value. We will show here an extrapolation procedure for the particular example of pure bcc Fe calculated with one atom per unit cell and spin polarization, with 10 000 **k**-points. As we can see in figure 2 the energy attains its converged value at RK_{max} around 10. The full curve in that figure is an exponential fit to the calculated cohesive energy:

$$E_{\text{atom}} - E_{\text{bcc Fe}} = E_{\text{cohesive}} = A - B\mathrm{e}^{-(k\cdot \mathrm{RK}_{\max})} \tag{1}$$

where A, B and k are constants. A represents the energy value for $RK_{max} = \infty$, that is, the total cell energy if it were calculated with an infinite number of plane waves. Therefore, the use of parameter A instead of the total energy calculated with any value of RK_{max} is a better estimate of the total energy per unit cell of the system and also provides an estimate of the calculation error. For this particular case we obtain $A_{\text{Fe}}^{\text{FERRO}} = (6.501 \pm 0.003)$ eV for the magnetic case and $A_{\text{Fe}}^{\text{PARA}} = (5.917 \pm 0.002)$ eV for the paramagnetic case, when the Fe atom energy is that given by the same code.

If the cell size increases to 36 atoms, as in the rest of the present paper, $RK_{max} = 10$ is beyond our computational capacity, and the use of equation (1), fitting the energies from calculations with RK_{max} between 7 and 8, could be very useful.

3. Analysis of existing experimental results

A number of experiments show that the relation between the logarithm of the diffusion coefficient (D) and the reciprocal of the absolute temperature (the so-called Arrhenius plot), which is normally linear for metals, deviates from linearity for ferromagnets.

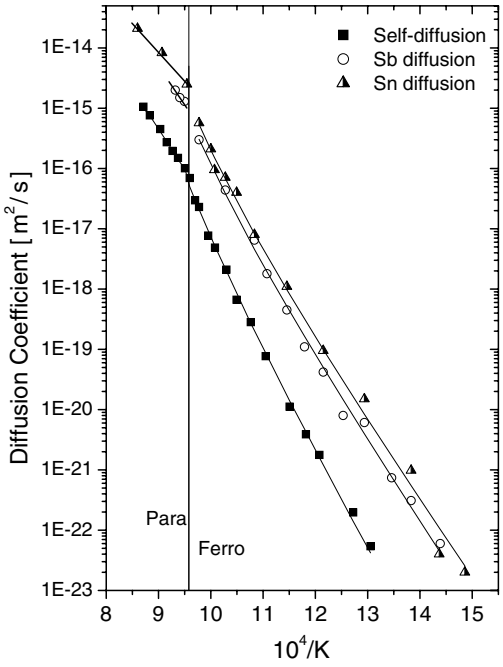

Figure 3. Arrhenius plots for Sn, Sb and self-diffusion in α-Fe. The curves are fits according to equation (7).

In the particular case of α-Fe, self-diffusion measurements performed by several authors [7, 1, 8] show a linear Arrhenius plot in the paramagnetic region but a break at the Curie temperature ($T_C = 1043$ K) and a soft upward curvature at lower temperatures in the ferromagnetic region, these values being lower than the ones extrapolated from the high temperature region. The same behaviour is observed in the diffusion of several solutes, when they are studied in an extended temperature range, as shown in figure 3.

An interpretation of the magnetic ordering effect on diffusion is possible assuming a vacancy mechanism for diffusion and also that the energy for vacancy formation and vacancy migration at any given temperature depends on the degree of magnetic order (i.e. spontaneous magnetization).

From the random walk theory, D for a vacancy mechanism is given by

$$D = \frac{f r^2 \Gamma_v C_v}{6} \tag{2}$$

where f is the correlation factor (for a vacancy mechanism, f is independent of temperature), r is the jump distance, Γ_v is the average jump frequency and C_v is the average vacancy concentration. These last two temperature dependent quantities are related to the migration and formation energy of vacancies, respectively. Ruch *et al* [2], extending early work by Girifalco [9], describe the effects of ordering on diffusion, using the spontaneous magnetization as the order parameter. The configurational energy in the case of a ferromagnet is taken as the Hamiltonian of a system of ions each having a resultant spin S_i so, considering only nearest neighbour interactions,

$$E_{ex} = -2J \sum_{(i,j)} S_i S_j. \tag{3}$$

Table 1. Diffusion parameters as obtained from experimental measurements.

	D_{0p} ($m^2\ s^{-1}$)	Q_p (eV)	α	αQ_p (eV)
Sn	6.0×10^{-6}	1.9 ± 0.2	0.23	0.44 ± 0.04
Sb	1.3×10^{-5}	2.1 ± 0.2	0.20	0.42 ± 0.04
Fe	2.7×10^{-4}	2.5 ± 0.1	0.16	0.41 ± 0.05
Co	—	—	0.23	0.50 ± 0.05
Cr	4.0×10^{-3}	2.8 ± 0.1	0.14	0.39 ± 0.04

Following a statistical mechanical treatment they finally arrive at

$$C_v = e^{-[E^0_{for}+(zJ/2)s^2]/kT} \qquad \text{and} \qquad \Gamma_v = \nu_{eff} e^{-E_m/kT} \tag{4}$$

where z is the coordination number and s is the ratio of the spontaneous magnetization at temperature T to that at 0 K (reduced magnetization) and has been experimentally determined by Crangle and Goodman [10]. E^0_{for} is the vacancy formation energy in a disordered crystal and E_m and ν_{eff} depend on the local atomic configurations. ν_{eff} is assumed to be independent of temperature and E_m is calculated as the static energy difference between the energy of an atom in the activated position for a diffusive jump and that of an atom in the adjacent equilibrium position. E_m is of the form

$$E_m = E^0_m + Cs^2 \tag{5}$$

where C is a constant and E^0_m is the migration energy for an atomic jump in a disordered (paramagnetic) crystal. The activation energy for diffusion in a paramagnetic crystal, Q_p, is $E^0_{for} + E^0_m$. If α is defined as

$$\alpha = \frac{C + \frac{1}{2}zJ}{Q_p} \tag{6}$$

and all the temperature independent constants are lumped into the pre-exponential factor D_0, the expression for the diffusion coefficient in a ferromagnet is given by

$$D(T) = D_0 \exp[-Q_p(1 + \alpha s^2)/RT]. \tag{7}$$

Note that α is an adimensional constant composed by two additive terms, one due to the variation in the formation energy ($\alpha_f = zJ/2$) and the other that in the migration energy ($\alpha_m = C$) due to magnetic ordering, both in units of Q_p; therefore equation (6) can also be expressed as

$$\alpha = \frac{\alpha_f + \alpha_m}{Q_p}. \tag{6'}$$

This model was applied to the self-diffusion [7, 1], and to that of Co [11], Cr [12], Sn [13] and Sb [14] in α-Fe, successfully. The parameters that fit equation (7) for each diffuser are given in table 1. The experimental diffusion coefficients for non-magnetic diffusers are shown in figure 3 together with the self-diffusion and with the model fitting. The percentage increment in the activation energy between the totally unaligned spins (paramagnetic state) and the totally aligned spins (ferromagnetic at 0 K), represented by the α parameter, varies from 14 to 25%. The value of αQ_p seems to be around 0.4 eV for all these elements except Co.

As we can see in table 1 and figure 3, this model describes the experimental results quite successfully. However, it is well known that a simple Ising model with only nearest neighbour interactions is a poor approximation to the ferromagnetic systems and becomes even worse if more neighbours are considered [15]. For example, the numerical value of α_f

Table 2. Calculated formation and migration energies for $RK_{max} = 7.4$.

	Ferromagnetic		Paramagnetic			
Diffuser	E_{for} (eV)	E_{mig} (eV)	E_{for} (eV)	E_{mig} (eV)	Q_p	αQ_p
Fe	2.57	0.80	1.55	0.44	1.99	1.38
Co	2.67	0.78	1.63	0.33	1.96	1.49
Cr	2.48	0.59	1.63	0.20	1.83	1.23
As	2.05	0.35	1.35	0.00	1.35	1.05
Sn	1.91	0.68	1.25	0.46	1.71	0.90
Sb	1.93	0.69	1.13	0.40	1.53	1.10

calculated theoretically for pure α-Fe by Ruch *et al* [2] is too low, 0.045 eV, compared with the value estimated from positron annihilation experiments [16]. Therefore, first-principles calculations are certainly necessary for a better understanding of the experimental results and of the phenomenological models.

4. Present calculations

4.1. Formation and migration energies

Table 2 reports the vacancy formation energies (E_{for}) calculated according to the following equation:

$$E_{for} = E_{34Fe+imp+vac} + E_{Fe} - E_{35Fe+imp} \tag{8}$$

where the first term is the energy of the cell with vacancy and impurity neighbours along the $\langle 111 \rangle$ direction, the second term is the energy per atom of pure bcc Fe and the last one is for a cell with only one substitutional impurity.

The migration energy (E_{mig}) was calculated as the difference between the energy of a system with the impurity in a substitutional site, with a vacancy as first neighbour (figure 1(a)), and that with the impurity in the saddle point configuration (figure 1(b)). In a few cases we made calculations for other positions for the impurity along the $\langle 111 \rangle$ path and found that the saddle point was always the energy maximum. The energy barrier shows a flat region near the maximum but never two maxima, as suggested by some empirical potential calculations [17].

The highest value of RK_{max} allowed by our computational facilities for all the cases studied was 7.4, and it was clear that convergence in RK_{max} had not been achieved. However, an interesting qualitative analysis could be performed. Magnetic solutions always have lower total energy than the paramagnetic ones, as expected. Also, the activation energies Q, that are the sums of the formation and migration energies, are lower in the paramagnetic case, as in the experimental results. This sustains the interpretation made in section 3 that a lattice stiffening due to the ferromagnetic order is the cause of the Arrhenius plot curvature.

αQ_p is almost the same for all the non-magnetic impurities, about 1 eV, while it is different for each of the magnetic impurities. αQ_p is the difference between the diffusion activation energy when all spins are aligned (at 0 K) and that of the paramagnetic situation. It is due to the magnetic interaction of the diffuser with the neighbour Fe atoms but also to the interaction among these. By looking at the spin densities inside the unit cell, one can understand why all non-magnetic impurities give almost the same value. Figure 4 shows the spin densities on the (110) plane for different impurities and it is clear that on this scale the magnetic impurities and the vacancies are identical; non-magnetic impurities behave as magnetic vacancies, so the

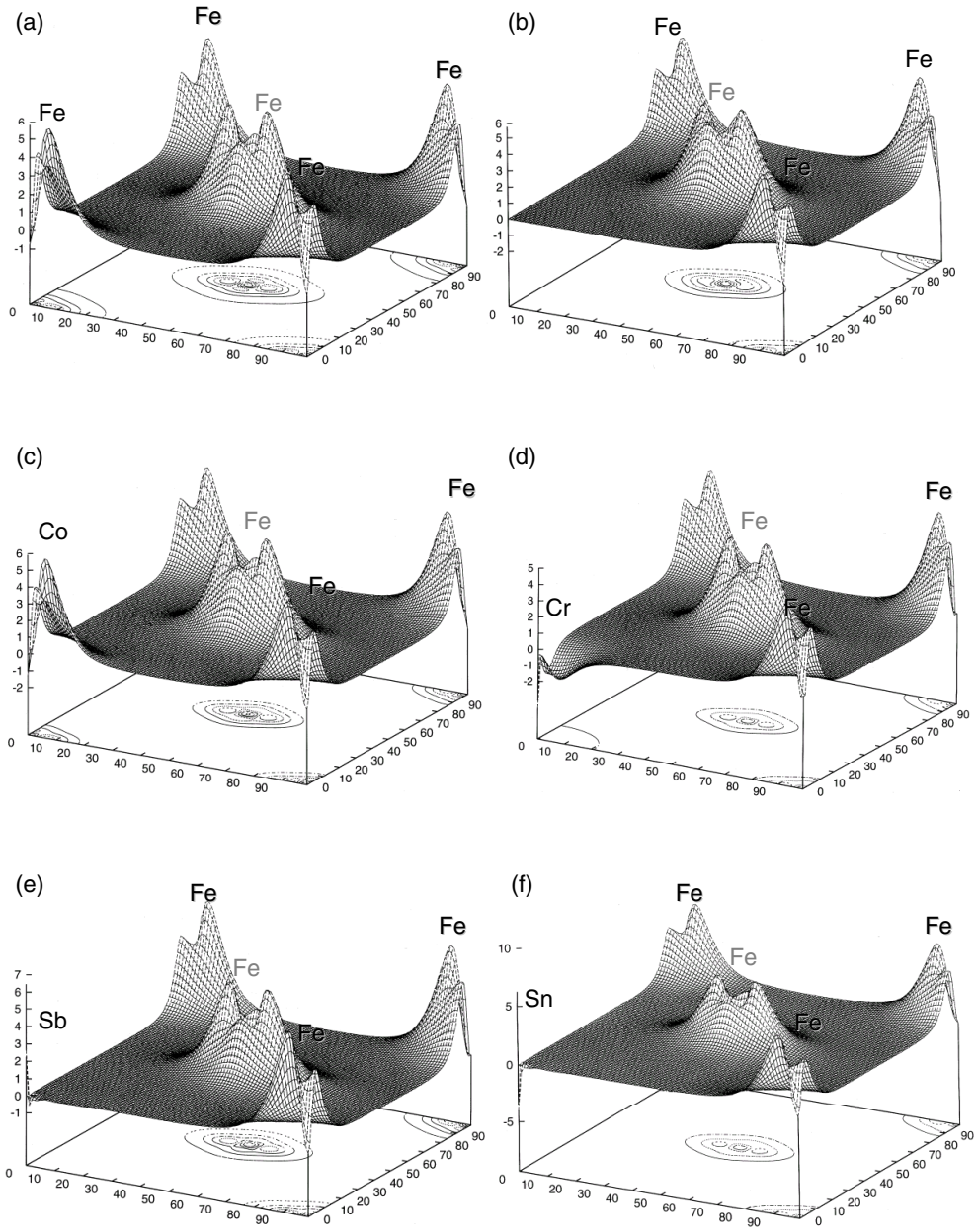

Figure 4. Spin densities on the [110] plane: (a) a perfect pure iron cell, (b) pure iron with a vacancy, ((c)–(f)) a lattice with the above-mentioned impurity in a substitutional position (Co, Cr, Sb and Sn respectively).

increment in the diffusion barrier is only due to the interaction among the Fe atoms involved in the diffusion jump.

For the impurities there are no positron annihilation data, only diffusion coefficients. Therefore E_{for} and E_{mig} cannot be obtained separately, but their sum, Q_{p}, for the paramagnetic region is given in table 1. The non-magnetic diffusers have a smaller Q_{p} and this is also obtained in the calculations. The measurement of As diffusion in α-Fe is still in progress in

Table 3. Magnetic moments (in Bohr magnetons).

	Impurity	Fe_{nn}	Interstitial	Cell
Impurity in Fe supercell				
Fe	2.30	2.30	−1.76	81.00
Co	1.80	2.43	−1.61	82.17
Cr	−1.79	2.36	−1.78	78.65
As	−0.05	2.29	−1.54	80.43
Sn	−0.08	2.29	−1.63	79.86
Sb	−0.07	2.23	−1.60	80.25
Impurity with a vacancy as next neighbour				
Fe	2.44	2.44	−1.16	79.62
Co	1.81	2.45	−0.99	79.79
Cr	−1.36	2.53	−1.36	76.57
As	−0.06	2.46	−1.12	78.19
Sn	−0.10	2.44	−1.01	77.52
Sb	−0.07	2.47	−1.22	77.63
Impurity at a saddle point				
Fe	2.39	2.45	−1.30	79.47
Co	1.82	2.48	−1.42	79.83
Cr	−1.96	2.51	−1.81	75.55
As	−0.06	2.50	−1.29	77.88
Sn	−0.08	2.48	−1.31	77.41
Sb	−0.07	2.49	−1.35−	77.66

our laboratory and experimental characteristics similar to those for Sn and Sb diffusion in α-Fe are being observed. Nevertheless, As is a singular element as it stabilizes and extends the bcc α-phase of Fe to higher temperatures even when present in small amounts [18]. This might be related to the surprising migration behaviour obtained in the calculations, that has been checked by changing the cell shape and the number of plane waves. The energies of a cell with As in a substitutional position (beside a vacancy) and in the saddle point configuration are the same, which indicates that it may also appear in the lattice as an interstitial. If this was the case, Q_p would no longer be the energy sum indicated in table 2 and a different calculation should be performed to obtain it.

When the impurity is a magnetic one, the interactions with the neighbouring Fe atoms depend on the magnetic moment of the impurity and different increments in the activation energy are observed. For Co, the increase in the diffusion barrier is even higher than for self-diffusion, given its strong interaction with the matrix, as we will see in the next section. When the diffusing impurity is Cr, which aligns antiferromagnetically with the Fe matrix, no large interaction is expected, so an αQ_p close to the non-magnetic diffuser is observed in the present calculations and also in the experimental measurements (see table 1).

4.2. Magnetic moments

Table 3 reports the magnetic moments inside the muffin tins and in the interstitial region obtained from our calculations. Co is the only impurity that increases the magnetic moment of the whole cell, although its magnetic moment is smaller than that of Fe. This fact has been known for a long time—it is even referred to in Kittel's book [19]; but it is nevertheless surprising. It is also surprising that the cell with a non-magnetic impurity or a vacancy has

a larger total magnetic moment than 35 times the bulk Fe moment =78.8 μ_B. This can be explained for the vacancy because when magnetic atoms are located on a surface their magnetic moment increases with respect to the bulk material due to a narrowing of the local densities of states—even more so if the surface atoms are different from the bulk ones and the epitaxy forces them to be further apart than in the corresponding bulk. Increased magnetization also appears close to voids and vacancies, as these again reduce the number of neighbours of the magnetic atom. For this reason we show in table 3 the magnetic moments of Fe atoms that are nearest neighbours to the vacancy.

The small magnetic moment of the non-magnetic impurities reported in table 1 is due to hybridization; it is aligned antiferromagnetically with respect to Fe. This is similar to what happens with the 4s and 4p electrons of Fe, those contributing most to the interstitial region of the cell. They interact preferentially with the majority 3d band of iron because it is closer in energy, and that induces a moment so small that is not seen in the spin density plots or in the corresponding densities of states. The cases of Cr and Mn are of course quite different; they are also aligned antiferromagnetically with respect to the host but the large magnetic moment comes from their incomplete 3d bands.

4.3. Extrapolation to $\mathrm{RK_{max}} = \infty$

As we pointed out in section 2, an exponential fit of the cell energy versus $\mathrm{RK_{max}}$ can be useful for extrapolation. In this section we apply this idea to the calculations performed in supercells. As

$$\alpha Q_p = (E_{for}^{FERRO} - E_{for}^{PARA}) + (E_{mig}^{FERRO} - E_{mig}^{PARA}), \tag{9}$$

using equation (8) and the definition of E_{mig}, we obtain

$$\alpha Q_p = [E_{34Fe+saddle} + E_{Fe} - E_{35Fe+imp}]^{FERRO} - [''']^{PARA} \tag{10}$$

where the first term in the bracket corresponds to the energy of a cell with an impurity at a saddle point, the third term has a substitutional impurity and $[''']^{PARA}$ represents the same bracket but for the paramagnetic energies. This expression requires only four supercell calculations for each $\mathrm{RK_{max}}$.

In the particular case of self-diffusion (imp = Fe), as $E_{35Fe+imp} - E_{Fe} = 35E_{Fe}$, only two supercell calculations are required; these are plotted in figure 5. The limiting value of αQ_p is obtained as

$$\alpha Q_p = [35A_{Fe} - A_{(34Fe+saddle)}]^{FERRO} - [35A_{Fe} - A_{(35Fe+saddle)}]^{PARA} \tag{11}$$

using the fitting parameters A for each case.

As can be appreciated in figure 6 (full curve), the extrapolated value of αQ_p is 0.5 eV, but the estimated error coming from the procedure of fitting the A parameters is 0.3 eV. The value measured directly by means of positron annihilation [16] is 0.4 ± 0.2 eV, and that obtained via diffusion coefficient measurements is 0.41 ± 0.05 eV, as listed in table 1. Although the numerical coincidence may be fortuitous, it is clear that small values of $\mathrm{RK_{max}}$ give too large estimates for αQ_p.

We have also extrapolated $E_{35Fe+vac}$, E_{for} and E_{mig} for self-diffusion for both magnetic and non-magnetic cases. These quantities have been measured separately, and there is a large dispersion between results from different authors and different methods. Most recent positron annihilation experiments [16] give $E_{for} = 2.0 \pm 0.2$ eV and 1.8 ± 0.1 eV for the ferromagnetic and paramagnetic cases respectively. Our numerical values, extrapolated for $\mathrm{RK_{max}} = \infty$, are 2.2 ± 0.3 and 1.6 ± 0.3 eV, almost within the experimental errors, although no lattice relaxation has been performed. For E_{mig} we obtain 0.5 ± 0.1 and 0.6 ± 0.1 eV respectively

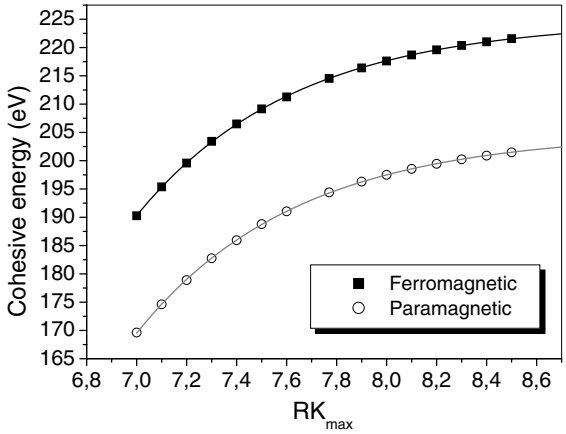

Figure 5. Calculated cohesive cell energy versus RK_{max} for a supercell with one Fe atom at a saddle point.

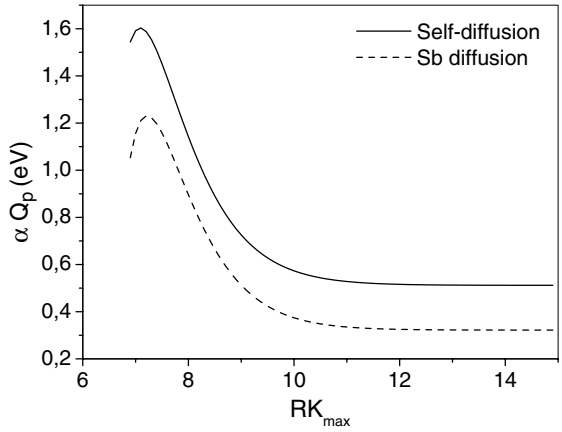

Figure 6. αQ_p versus RK_{max} for self-diffusion and Sb diffusion in α-Fe.

and the experiments give 0.55 [20] for the ferromagnetic case. The magnetic calculations can be compared with those of other authors collected in table 4 of [3] and the agreement is very good, even though no relaxation was performed in our case.

When we tried to introduce relaxation by displacing the Fe atom in the ⟨111⟩ direction from its equilibrium position to the neighbour vacancy position, very different results were obtained from spin-polarized and non-spin-polarized calculations. For the spin-polarized case a normal 1% relaxation in the position, a vacancy formation energy increasing about 10% and a plateau at the top of the barrier (instead of a double peak, as reported from some pair potential calculations) were obtained. In contrast, for the non-spin-polarized case an unusually large displacement from the equilibrium position (about 10%) was observed. This may be due to the limitations in size and shape of our unit cell, combined with the fact that non-magnetic Fe is not the stable state at 0 K. For this reason we discarded the possibility of including relaxation in our calculations.

The same extrapolation procedure was applied as an example to the diffusion of Sb in Fe, although with a smaller RK_{max}, which increases the error of the extrapolation. It gives for the

cohesive energies $A_{(35\text{Fe+imp})} = 228.781 \pm 0.2$ eV and $A_{(34\text{Fe+saddle})} = 220.289 \pm 0.3$ eV for spin-polarized calculations whereas for non-spin-polarized calculations the values are $A_{(35\text{Fe+imp})} = 210.498 \pm 0.3$ eV and $A_{(34\text{Fe+saddle})} = 202.911 \pm 0.2$ eV. If the A values are used in equation (9) instead of the energies for $\text{RK}_{\text{max}} = 7.4$, the value of αQ_{p} is reduced to 0.35 eV. Although the error in this case is very large, the same trend as in self-diffusion is observed (see figure 6, dashed curve). We conclude that the assumption often made in the literature, that energy differences between calculations performed for the same RK_{max} are almost independent of this value, is no longer valid when the quantities of interest are as small as in the present work.

5. Conclusions

Ab initio calculations of the vacancy formation and migration energies in iron with different impurities have been performed, and qualitative agreement with diffusion experiments over an extended temperature range has been obtained. Calculations were done both in the ferromagnetic and paramagnetic states, and although they are both at 0 K it is clear that the spin alignment produces a lattice stiffening and diffusion is therefore more difficult. The magnetic moments of iron atoms near the vacancies are increased appreciably. We have also shown that better quantitative agreement with experimental results is achieved by using an extrapolation to an infinite number of plane waves.

Different non-magnetic impurities have different activation energies, but the increase due to magnetic ordering is approximately constant, which is not the case for the magnetic impurities.

Acknowledgment

We thank Dr Roberto Pasianot for very carefully reading this manuscript.

References

[1] Iijima Y, Kimura K and Hirano K 1988 *Acta Metall.* **36** 2811
[2] Ruch L, Sain D R, Yeh H L and Girifalco L A 1976 *J. Phys. Chem. Solids* **37** 649
[3] Domaine C and Becquart C S 2001 *Phys. Rev.* B **65** 024103 and references therein
[4] Ackland G J, Bacon D J, Calder A F and Harry T 1997 *Phil. Mag.* A **75** 713
[5] Blaha P, Schwartz K and Luitz J 1997 *WIEN97* (Vienna: Vienna University of Technology) Improved and updated UNIX version of the original copyrighted WIEN code, which was published by Blaha P, Schwartz K, Sorantin P and Trickey S B 1990 *Comput. Phys. Commun.* **59** 388
[6] Perdew J P, Ernzerhof M and Burke K 1996 *J. Chem. Phys.* **105** 8982
[7] Hettich G, Mehrer H and Maier K 1977 *Scr. Metall.* **11** 795
[8] Lubbehusen M and Meher H 1990 *Acta Metall.* **38** 283
[9] Girifalco L A 1962 *J. Phys. Chem. Solids* **23** 1171
[10] Crangle J and Goodman G M 1971 *Proc. R. Soc.* A **321** 477
[11] Iijima Y, Kimura K, Lee C and Hirano K 1993 *Mater. Trans. JIM* **34** 20
[12] Lee C, Iijima Y, Hiratani T and Hirano K 1990 *Mater. Trans. JIM* **31** 255
[13] Torres D N, Pérez R A and Dyment F 2000 *Acta Metall.* **48** 2925
[14] Pérez R A, Torres D and Dyment F 2004 *Appl. Phys.* A at press and references therein
[15] Morán S, Ederer C and Fähnle M 2003 *Phys. Rev.* B **67** 12407
[16] De Shepper L, Seger D, Dorikens-Vanpraet L, Dorikens M, Knuyt G, Stals L M and Moser P 1983 *Phys. Rev.* B **27** 5257
[17] Mendelev M I, Han S, Stolovitz D J, Ackland G J, Sun D Y and Asta M 2003 *Phil. Mag.* **83** 3977
[18] Okamoto H 1993 *Monograph Series on Alloy Phase Diagrams: Phase Diagram of Binary Iron Alloys* 1st edn, vol 9, ed H Okamoto (Metals Park, OH: ASM International) p 29
[19] Kittel C 1986 *Introduction to the Solid State Physics* 6th edn (New York: Wiley) chapter 11, p 437
[20] Vehanen A, Hautojärvi P, Johansson J, Yli-Kauppila J and Moser P 1982 *Phys. Rev.* B **25** 762